Journal of Physics: Conference Series

Selective bond scission in formic acid by low-energy electrons

Selective bond scission in formic acid by low-energy electrons

Brandon Griffin,[1] Ali Moradmand,[2] Joshua Williams,[1] Ali Belkacem,[3] Thomas N Rescigno,[3] Cynthia Trevisan,[2] C William McCurdy,[3,4] Thorsten Weber[3] and Daniel S Slaughter[3]

[1]Department of Physics, University of Nevada Reno, Reno, Nevada 89557, USA
[2]Department of Sciences and Mathematics, California Maritime Academy, Vallejo, California 94590, USA
[3]Chemical Sciences Division, Lawrence Berkeley National Laboratory, 1 Cyclotron Rd, Berkeley, CA 94556, USA
[4]Department of Chemistry, University of California, Davis, CA 95616

E-mail: DSSlaughter@lbl.gov

Abstract. We report recent results of mass-resolved anion fragment momentum imaging experiments to investigate dissociative electron attachment to formic acid, for incident energies between 5 eV and 9 eV. A remarkable site-selectivity is found for a resonance at 8.5 eV by comparing anion fragment yields for two deuterated isotopologues of formic acid. This results in an H^- fragment from the O-H bond of the transient anion, with negligible contribution from C-H break. In contrast, a lower-energy resonance at 7.1 eV dissociates by C–H or O–H break to produce H^- and the neutral radicals HOCO or HCOO.

1. Introduction

Low energy electrons are well-established to have importance in chemical processes initiated by ionizing radiation [1]. This is because electrons are produced in high abundance with energies in the range for resonances to drive molecular dissociation by inelastic scattering and dissociative electron attachment (DEA). In DEA, the energy of a free electron is efficiently converted into vibrational kinetic energy and dissociation into two or more atomic or molecular fragments [2]. The process necessarily involves a strong coupling between electronic and nuclear motion, resulting in rich nonadiabatic dynamics such as conical intersections [3] or electron transfer [4] between electronic states of the transient anion, that are very difficult, if not impossible to model without detailed experimental data. In molecules with few degrees of symmetry, site selectivity may be observed where dissociation favors one moiety within the transient anion over another, depending on the electron attachment energy.

Formic acid (HCOOH), being the simplest organic acid, is a useful model system in developing a fundamental understanding electron-driven chemistry. It also has several important applications in nature and industry. The first organic acid to be observed in the interstellar medium [5, 6, 7], formic acid continues to attract intense interest as a chemical precursor or an intermediate species in the abiotic synthesis [8, 9] of biologically-relevant molecules. In Earth's atmosphere, the chemistry of formic acid is relevant to solubilities and reaction rates of natural

and synthetic pollutants [10]. In energy transport applications, formic acid has been identified as a high-efficiency fuel for direct liquid fuel cells [11].

A low-energy shape resonance in formic acid has been the subject of several investigations, primarily focusing on the mechanism of electron attachment around 1.8 eV. Several theoretical studies produced two possible mechanisms: electron attachment to a σ^* resonance [12, 13, 14, 15] that directly dissociated to $HCOO^- + H$; or attachment to a π^* resonance [16, 17, 18], followed by C–H bending out-of-plane, to stabilize the anion electronically and couple to a σ^* state to produce $HCOO^- + H$. The subsequent experimental investigation of Janeckova *et al.* [19] measured a relatively weak dependence of the DEA cross section on substitution of the C–H hydrogen with deuterium, supporting the direct mechanism with no out-of-plane C–H bending. In this work, we examine two different resonances between 5 eV and 9 eV that produce H^-, O^- and OH^-. The resonances have been studied previously by measurements of the mass-resolved ion yields and their incident electron energy-dependence [20, 21, 22, 23]. In this contribution we focus on the site selectivity of DEA leading to H^- loss from the formyl or hydroxyl moieties.

2. Experimental methods

A DEA reaction microscope was used to measure the mass-resolved anion fragment yields and initial momentum after dissociative electron attachment. The technique has already been described elsewhere [24, 3], so only the most important details are included here. The experiments employ an energy-tunable, pulsed electron beam that is directed orthogonally with the time-of-flight axis of a momentum imaging spectrometer. Deuterated formic acid (HCOOD or DCOOH, 98% isotopologue purity) was obtained from Sigma Aldrich and degassed in the vacuum chamber sample manifold by a series of freeze-pump-thaw cycles. Formic acid vapor was admitted into the ultra-high vacuum chamber by heated (80°C) stainless tubing and collimated by a long stainless steel capillary of 0.3 mm inner diameter to form the gas target. The tubing and vacuum apparatus were baked to >120° for 48 hours beforehand to reduce the presence of water below significant concentrations, as determined by the rate of H^- or D^- from H_2O or D_2O, respectively, at the $^2B_1$ resonance energy of 6 eV. The pure formic acid effusive beam was maintained at low pressure conditions, <2 Torr within the tubing upstream of the capillary, to ensure negligible contributions from formic acid dimers [25]. The collision region, defined by the intersection of the molecular and electron beams, was aligned between the first two parallel electrodes of the anion fragment momentum imaging spectrometer. The first electrode of the anion spectrometer was pulsed following a delay from the electron gun pulse, extracting negative ion fragments into the spectrometer at a system repetition rate of 50 kHz. A magnetic field coaxial to the electron gun allowed the separation of anions from the scattered electron background and assisted in the low energy electron beam transport and collimation. The electron beam was characterized, using the sharp increase in O^- from CO_2 around its 4.0 eV DEA threshold, to determine the energy spread of 0.5 eV (full width at half maximum). The electron beam mean energy was calibrated by the same O^- onset curve and determined within ±0.1 eV for each experiment.

The momentum-imaging anion spectrometer produced 12 V/cm anion extraction and acceleration fields, followed by a position-focusing lens to map the initial momentum of anion fragments onto the position and time-sensitive anion detector. The detector consisted of a grid electrode for anion post-acceleration and a pair of 75 mm diameter chevron microchannel plates that amplified each detected particle onto a two-layer delay line anode, allowing the event-by-event acquisition of the 3-dimensional momentum of each ion, encoded in the time and position of each ion hit. Extensive shielding of the detector and spectrometer prevented most of the background scattered electrons from entering the spectrometer or hitting the detector. In the list-mode data record, the 3-dimensional momentum of each detected ion fragment was stored, allowing for both on-the-fly and offline analysis.

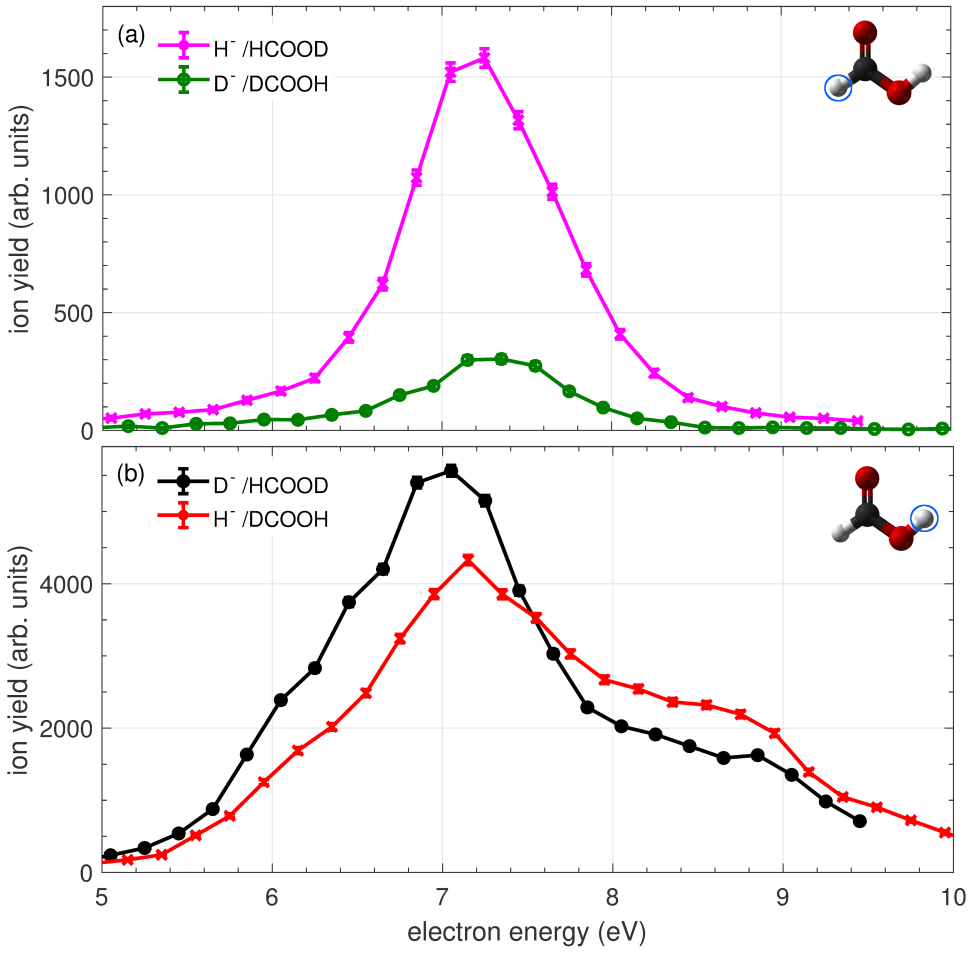

Figure 1. Incident electron energy dependence of relative yields of anion fragments for dissociative electron attachment to deutrated formic acid. (a) C–H break measured by H^- from HCOOD and D^- yield from DCOOH. (b) O–H break measured by H^- from DCOOH and D^- yield from HCOOD. Error bars represent plus/minus one standard deviation and, where they not visible, they are smaller than the data point symbols.

Momentum imaging experiments require several hours of data collection to achieve acceptable statistical uncertainties in the momentum-differential data. To produce mass-resolved anion fragment yields, the same experimental approach was employed for a much shorter time of 120 s per incident electron energy, to reduce the systematic uncertainties originating from instabilities in the molecular beam density. The anion fragment yields are not calibrated to an absolute scale and the relative yields for each of the two target molecules, HCOOD and DCOOH, were measured in different experimental runs under very similar conditions. Therefore the yields for each target are only approximately normalized to the same arbitrary scale, with the scale uncertainty for each target molecule estimated to be ±50%.

3. Results

The relative yields of anions produced by C–H and O–H break, measured as a function of incident electron energy are presented in figure 1.

A single narrow peak in the H^- (D^-) yield is measured for C–H (C–D) bond scission, having

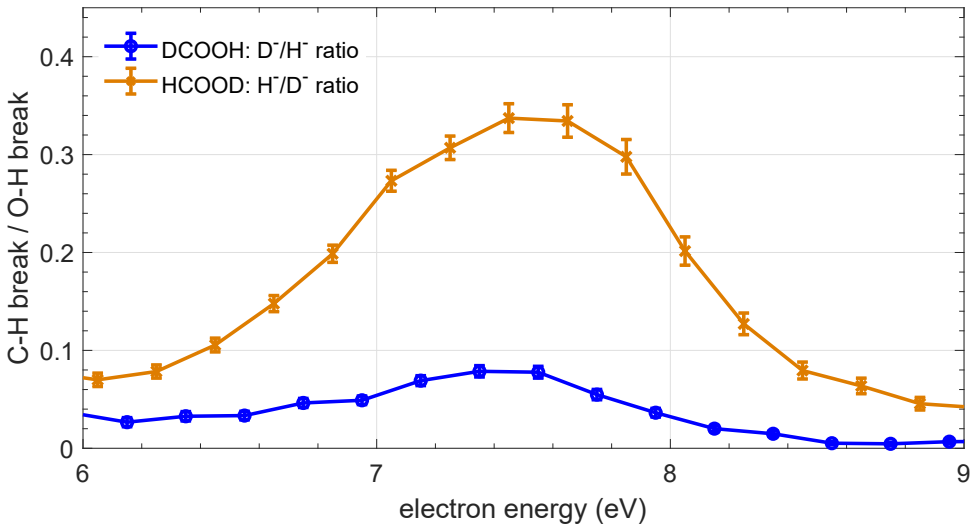

Figure 2. Yield fractions at the 7.1 eV resonance, D^-/H^- fraction from DCOOH and H^-/D^- fraction from HCOOD, showing a higher rate of O–H (or O–D) break compared to C–H (or C–D) break in both formic acid isotopologues.

a width of about 1 eV and symmetric shape about its maximum at 7.1 eV (figure 1 (a)). A peak at the same energy also occurs in the O–H break product yield (figure 1 (b)), however the shape is considerably different and about 0.5 eV broader than the corresponding C–H peak. A higher energy shoulder in the H^- (D^-) yield for O–H (O–D) scission is prominent at about 8.5 eV. Determining the absolute DEA cross sections from the present anion yields is not possible in the present experiments, however the relative yields of anion fragments reveal a significant isotope effect for C–H dissociation. On comparison of the DCOOH data in figures 1 (a) and (b), C–D scission is considerably less-favorable than O–H scission, and this is also the case, to a lesser extent, for HCOOD. This effect is quantified in the relative yields shown in figure 2, where we compare the ratio of C–H to O–H dissociation for each molecule. Specifically, the fractions (C–D break)/(O–H break) for DCOOH and (C–H break)/(O–D break) for HCOOD show that, over the entire energy range, O–H break is favored over C–D break, and O–D break is favored over C–H break. Near the 7.1 eV resonance, C–H break contributes to a fraction of about 1/3 to the total ion yield for formic acid deuterated at the hydroxyl moiety (HCOOD), C–D break contributes to 1/12 of the total ion yield for the formyl-deuterated isotopologue DCOOH.

To better identify the transient anion resonances associated with the incident electron energy-dependent structures in the DEA product yields, we examine the measured three-dimensional momentum images in figure 3 for the fragment anions produced at a few relevant incident electron energies. Each image displays the momentum of D^-, originating from the site indicated by the inset cartoon of each panel, in the laboratory frame defined by the electron beam direction. The longitudinal or transverse coordinates correspond to anion fragment dissociation in the same direction or orthogonal to the electron beam, respectively. To display ions emitted within a uniform solid angle, each image is extracted from the full momentum-space Newton sphere by extracting an inverted conical 30° slice [24].

4. Discussion

The anion yields of figure 1 show structures corresponding to DEA involving at least two distinct transient anion resonances. At least 11 excited electronic states [26] exist between 7.5 eV and

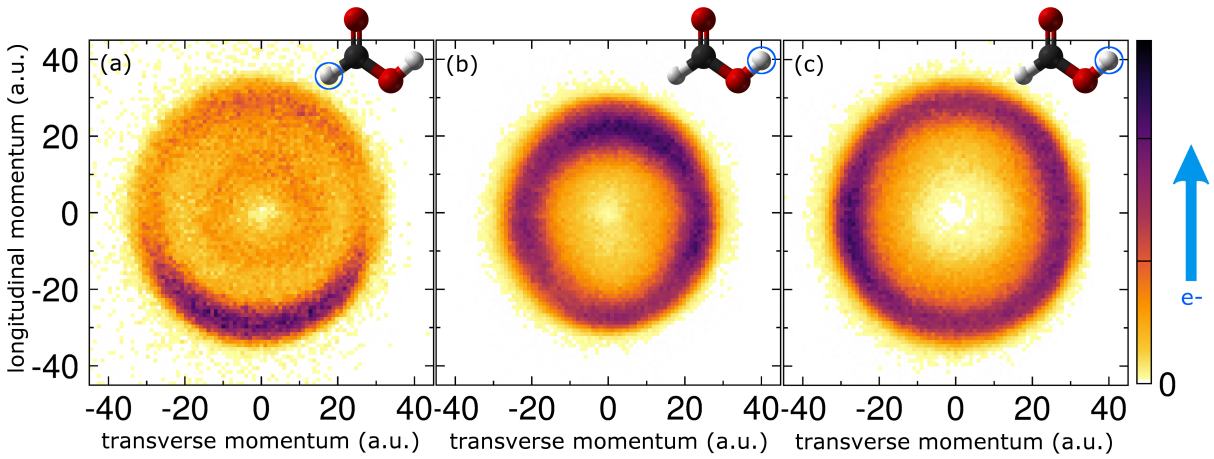

Figure 3. Momentum images of the D^- fragment for formic acid deuterated at (a) the formyl moiety (DCOOH), for 7.6 eV incident electron energy, and the hydroxyl moiety (HCOOD) for (b) 7.2 eV and (c) 8.5 eV incident electron energies. The incident electron direction is shown by an arrow on the right and the units of the linear intensity scale are arbitrary.

9 eV above the ground electronic state of formic acid. Any of them could be considered as possible parents of core-excited shape or Feshbach resonances. The minimum energy geometry of neutral formic acid in the ground electronic state is the *cis* (or *anti*) isomer, and the *trans* (or *syn*) isomer is 169 meV higher in energy [26]. For the moderate molecular beam temperatures of the present experiments, any contributions from the *trans* isomer are expected to be negligible, however other structural transformations may occur in the excited anion states. An investigation of these dynamics will require challenging resonance electronic structure calculations, which are beyond the scope of the present work. The peak yields for C–H and O–H scission are both around 7.1 eV, indicating a common resonance that produces different products, hydrocarboxyl radical (HOCO) and formyloxyl radical (HCOO), respectively, in two distinct reaction channels:

$$\mathrm{HCOOH} + \mathrm{e}^- \rightarrow \mathrm{HCOOH}^- \rightarrow \mathrm{H}^- + \mathrm{HOCO} \quad (1)$$

$$\mathrm{HCOOH} + \mathrm{e}^- \rightarrow \mathrm{HCOOH}^- \rightarrow \mathrm{H}^- + \mathrm{HCOO} \quad (2)$$

The adiabatic dissociation limits have already been determined to be 3.43±0.1 eV for reaction 1 and 3.79±0.23 eV for reaction 2 [20, 22]. The total kinetic energy release (KER) in the assumed two-body fragmentation can be extracted from the momentum images of figure 3, and it was found that the KER distributions span 2 to 4 eV for reaction 1 and 3 to 4 eV for reaction 2. The equilibrium geometry of *cis*-HOCO is somewhat similar to formic acid [27, 26], however it is known to have small barriers of about 1 eV to dissociation into CO + OH or CO_2 + H [28]. HCOO has at least three low-lying excited electronic states [29, 30] that could be accessible by 7 eV and 8.5 eV dissociative electron attachment, and they may decay dissociatively to H + CO_2.

The momentum image in figure 3(a), corresponding to the HOCO product channel (reaction 1), displays a broad peak in the backwards direction, opposite to the incident electron direction. In contrast, the HCOO product channel (reaction 2) has a minimum in the backwards direction at the lower-energy resonance in figure 3(b), and is more isotropic for the 8.5 eV resonance in figure 3(c). While we cannot rule-out three distinct electron attachment resonances contributing to these observations, the present fragment momentum measurements are consistent with electron attachment to a narrow core-excited resonance at 7.1 eV, which dissociates by C–H

scission (reaction 1), and in a more complex process, to dissociation by O–H scission. The latter process may involve a more rapid stabilization of the transient anion, allowing DEA to compete more favorably with autodetachment and produce higher anion yields. The second resonance around 8.5 eV is expected to have a completely different molecular-frame electron attachment amplitude [3], resulting in the distinctly isotropic momentum ring in figure 3(c). An additional diffuse ring is also revealed for momenta <15 a.u. in figure 3(a). The shape of this feature was found to be insensitive to incident electron energies, suggesting that the origin may be a 3-body dissociation channel, possibly due to one or more higher-energy excited anion states.

5. Summary and outlook

Site-selectivity is observed in dissociative electron attachment in deuterated formic acid (HCOOD or DCOOH), where H^- or D^- is produced by breaking the C–H or C–D bond, respectively, in one DEA resonance centered at 7.1 eV. A second higher-energy resonance at about 8.5 eV produces no significant anions by C–H break, but both resonances produce H^- or D^- by breaking the O–H or O–D bond in DCOOH or HCOOD, respectively. Electron scattering calculations are needed to determine the molecular-frame electron attachment amplitudes in the molecular frame. Paired with the measurements presented here, a more complete analysis will then be possible to unravel the possible dissociation pathways involving hydrocarboxyl or formyloxyl neutral radicals.

Acknowledgments

This work is supported by the U.S. DOE Office of Basic Energy Sciences, Division of Chemical Sciences, Geosciences and Biosciences under contract DE-AC02-05CH11231. BG and JW acknowledge support from the National Science Foundation Grant No. NSF-PHY-1807017.

References

[1] Alizadeh E, Orlando T M and Sanche L 2015 *Annu. Rev. Phys. Chem.* **66** 379–398
[2] Fabrikant I I, Eden S, Mason N J and Fedor J 2017 *Adv. At. Mol. Opt. Phys.* vol 66 ed Arimondo E, Lin C C and Yelin S F (Academic Press) pp 545–657
[3] Slaughter D S, Belkacem A, McCurdy C W, Rescigno T N and Haxton D J 2016 *J. Phys.* B*: At. Mol. Opt. Phys.* **49** 222001
[4] Rescigno T N, Trevisan C S, Orel A E, Slaughter D S, Adaniya H, Belkacem A, Weyland M, Dorn A and McCurdy C W 2016 *Phys. Rev.* A **93** 052704
[5] Zuckerman B, Ball J A and Gottlieb C A 1971 *Astro. J.* **163** L41
[6] Bennett C J, Hama T, Kim Y S, Kawasaki M and Kaiser R I 2010 *Astrophys. J.* **727** 27
[7] Millar T J, Walsh C and Field T A 2017 *Chem. Rev.* **117** 1765–1795
[8] Becker S, Thoma I, Deutsch A, Gehrke T, Mayer P, Zipse H and Carell T 2016 *Science* **352** 833–836
[9] Orgel L E 2010 *Crit. Rev. Biochem. Mol. Biol.* **39** 99–123
[10] Millet D B, Baasandorj M, Farmer D K, Thornton J A, Baumann K, Brophy P, Chaliyakunnel S, de Gouw J A, Graus M, Hu L, Koss A, Lee B H, Lopez-Hilfiker F D, Neuman J A, Paulot F, Peischl J, Pollack I B, Ryerson T B, Warneke C, Williams B J and Xu J 2015 *Atmospheric Chem. Phys.* **15** 6283–6304
[11] Ong B C, Kamarudin S K and Basri S 2017 *Int. J. Hydrogen Energy* **42** 10142–10157
[12] Gallup G A, Burrow P D and Fabrikant I I 2009 *Phys. Rev.* A **79** 042701
[13] Rescigno T N, Trevisan C S and Orel A E 2009 *Phys. Rev.* A **80** 046701
[14] Gallup G A, Burrow P D and Fabrikant I I 2009 *Phys. Rev.* A **80** 046702
[15] Gallup G A 2013 *Phys. Rev.* A **88** 052705
[16] Gianturco F A and Lucchese R R 2004 *New J. Phys.* **6** 66
[17] Trevisan C S, Orel A E and Rescigno T N 2006 *Phys. Rev.* A **74**
[18] Rescigno T N, Trevisan C S and Orel A E 2006 *Phys. Rev. Lett.* **96**
[19] Janekov R, Kubala D, May O, Fedor J and Allan M 2013 *Phys. Rev. Lett.* **111** 213201
[20] Pelc A, Sailer W, Scheier P, Probst M, Mason N J, Illenberger E and Märk T D 2002 *Chem. Phys. Lett.* **361** 277–284
[21] Pelc A, Sailer W, Scheier P, Mason N and Mrk T 2002 *Eur. Phys. J.* D **20** 441–444
[22] Prabhudesai V S, Nandi D, Kelkar A H, Parajuli R and Krishnakumar E 2005 *Chem. Phys. Lett.* **405** 172–176

[23] Ptasińska S, Bass A D and Sanche L 2008 *J. Phys.: Conf. Ser.* **115** 012018
[24] Adaniya H, Slaughter D S, Osipov T, Weber T and Belkacem A 2012 *Rev. Sci. Instrum.* **83** 023106
[25] Allan M 2006 *J. Phys.* B*: At. Mol. Opt. Phys.* **39** 2939–2947
[26] Leach S, Schwell M, Dulieu F, Chotin J L, Jochims H W and Baumgärtel H 2002 *Phys. Chem. Chem. Phys.* **4** 5025–5039
[27] Clements T G, Continetti R E and Francisco J S 2002 *J. Chem. Phys.* **117** 6478–6488
[28] Johnson C J, Harding M E, Poad B L J, Stanton J F and Continetti R E 2011 *J. Am. Chem. Soc.* **133** 19606–19609
[29] Kim E H, Bradforth S E, Arnold D W, Metz R B and Neumark D M 1995 *J. Chem. Phys.* **103** 7801–7814
[30] Zou L, Li J, Wang H, Ma J and Guo H 2015 *J. Phys. Chem.* A **119** 7316–7324